Interface Structure and Radiation Damage Resistance in Cu-Nb Multilayer Nanocomposites

M. J. Demkowicz,* R. G. Hoagland, and J. P. Hirth
Los Alamos National Laboratory, Los Alamos, New Mexico 87545, USA
(Received 13 November 2007; published 1 April 2008)

We use atomistic simulations to show that upon removal or insertion of atoms, misfit dislocations in Cu-Nb interfaces shift between two adjacent planes, forming pairs of extended jogs. Different jog combinations give rise to interface structures with unlike densities but nearly degenerate energies, making Cu-Nb interfaces virtually inexhaustible sinks for radiation-induced point defects and catalysts for efficient Frenkel pair recombination.

DOI: 10.1103/PhysRevLett.100.136102 PACS numbers: 68.35.−p, 61.72.J−, 61.72.Lk, 61.80.−x

Although interfaces comprise <0.01% of the volume of a polycrystalline solid with micron-sized grains, they play a decisive role in determining its mechanical, electrical, thermal, and diffusion properties [1]. In a polycrystal with nanometer-sized grains interfaces account for 15%–30% of the material and often govern its behavior entirely, leading to dramatic effects like elevated strength [2,3], superplasticity [4], and suppression of fatigue [5]. Understanding of the physical basis of these phenomena is at a fledgling stage and requires a detailed knowledge of interface structure and properties.

We use atomistic simulations to investigate one of the interface-governed behaviors exhibited by multilayer nanocomposites of Cu and Nb with constituent layers 4 nm in thickness or less [5–7], namely, their substantially enhanced resistance to radiation damage compared to pure Cu or Nb [8,9]. We show that due to their distinctive structure, flat Cu-Nb interfaces do not support compact, well-localized point defects, which are the primary form of radiation damage in crystals [10]. Instead, these interfaces can accumulate large fluxes of vacancies and interstitials and enhance their recombination, allowing Cu-Nb nanocomposites to persist in a damage-free steady state even when driven out of equilibrium by intense particle radiation. The connections between structure and properties found here suggest the existence of an entire class of radiation damage-reducing interfaces, of which Cu-Nb is but one representative.

Model Cu-Nb bilayers are constructed in the experimentally observed Kurdjumov-Sachs (KS) orientation relation [11], in which a Cu {111} plane neighbors a Nb {110} plane and an interfacial Cu ⟨110⟩ direction lies parallel to a Nb ⟨111⟩ direction. The constituent Cu and Nb layers are 4 nm thick, have periodic boundaries in the interface plane, and terminate in free surfaces away from the interface. Remarkably, two distinct flaw-free interface atomic configurations satisfy these conditions [12]. One, termed KS_1, is obtained by simply joining fcc Cu and bcc Nb, as shown in Fig. 1(a). In the other—KS_2, Fig. 1(b)—the atomic layer of Cu immediately adjacent to Nb is homogeneously strained and rotated with respect to a perfect Cu {111} plane, reducing its areal density by ~0.5%. The structure of this strained atomic layer—named the "α geometry"—depends solely on the interface orientation relation and lattice parameters of Cu and Nb. The atomic layer itself is called Cu^{α}. Unlike KS_1, KS_2 contains two interfaces as shown in Fig. 1(b): Cu^{α}-Nb between Cu^{α} and the adjacent Nb {110} plane and Cu-Cu^{α} between Cu^{α} and the neighboring perfect Cu {111} plane. Both KS_1 and KS_2 prove stable and energetically nearly degenerate when relaxed using an embedded atom potential [13] constructed specifically to model the Cu-Nb system [12]. The difference in energies between them depends primarily on interface geometry and only weakly on the potential.

In atomistic simulations, interface misfit dislocations [1] can be found using disregistry analysis [14], as exemplified in previous work on Cu-Ni and Cu-Ag [2]. In this study, a reference state is chosen in which all close-packed Cu and Nb planes parallel to the interface are strained to be in the α geometry, like Cu^{α} in KS_2. Two sets of parallel misfit dislocations are found in the Cu-Nb interface of KS_1 and one set is found in each of the two interfaces in KS_2 (Cu^{α}-Nb and Cu-Cu^{α}). Dislocations inside KS_1 and in Cu^{α}-Nb of KS_2 are, respectively, shown in Figs. 1(a) and 1(b) by the locations of atoms in the interfacial Cu plane that neighbor on dislocation cores. Dislocations in Cu-Cu^{α} of KS_2 are shown in Fig. 1(b) by the locations of atoms with local hcp stacking in the perfect Cu {111} plane adjacent to Cu^{α}.

Figure 1 also gives the Burgers vectors $\vec{b}$ of all the dislocation sets found in KS_1 and KS_2. Set 1 in KS_1 has predominantly screw character while set 2 is mostly edge. Comparison of these misfit dislocation sets with those found in KS_2 demonstrates an intimate relationship between KS_1 and KS_2: while dislocation set 2 resides between interfacial Cu and Nb planes in both configurations, dislocation set 1 can exist either in the Cu-Nb interface of KS_1 or it can shift by one atomic plane into the neighboring Cu layer, creating the Cu-Cu^{α} interface and, therefore, KS_2. The geometry of Cu^{α} in KS_2 is a direct consequence of the difference in location of misfit dislocation set 1: when these dislocations shift from the Cu-Nb interface into the neighboring Cu layer, the intervening atomic plane

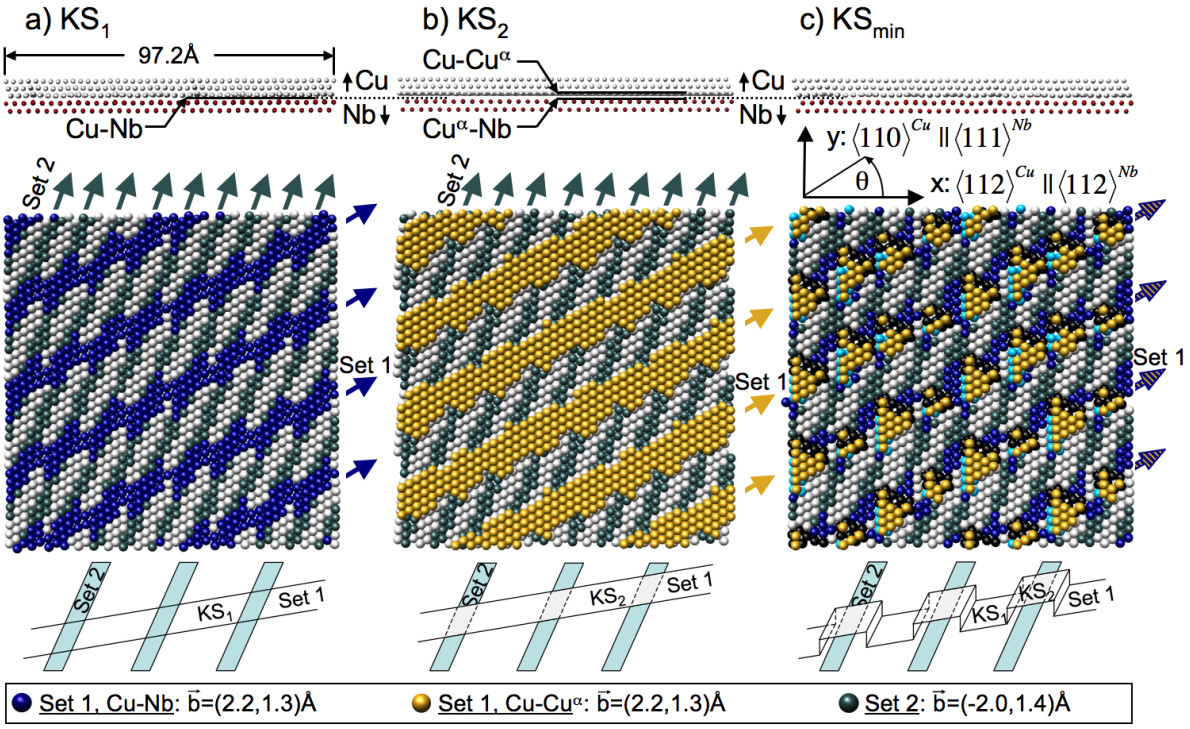

FIG. 1 (color online). Set 1 misfit dislocations lie in (a) the Cu-Nb plane in KS_1, (b) the Cu-Cu$^\alpha$ plane in KS_2, and (c) weave between these two planes in KS_{min}. Set 2 misfit dislocations lie in the Cu-Nb plane in all three interface configurations. The relative arrangement of misfit dislocations in these interfaces is illustrated in the schematics above the legend.

acquires the coherency strain that would have been annihilated by misfit dislocation set 1.

The ability of dislocation set 1 to reside in two neighboring atomic planes has dramatic consequences for the behavior of point defects near Cu-Nb interfaces. Figures 2(a) and 2(c) show the arrangement of an interfacial Cu plane of KS_1 upon removal and insertion of an atom, respectively, followed by molecular dynamics annealing at 300 K for 10 ps and potential energy minimization. Unlike in fcc Cu, removal (insertion) of an interface Cu atom in KS_1 does not lead to the formation of a compact vacancy (interstitial). Instead, the interfacial Cu plane in the vicinity of the removed or inserted atom undergoes reconstruction, resulting in an extended defect arrangement. Neighboring interfacial Cu atoms in this arrangement form rings with 5, 4, or 3 members. Atoms in Figs. 2(a) and 2(c) are colored by the size of the largest ring of which they are a part. Burgers circuits constructed around clusters of 4- and 5-member rings using perfect KS_1 as the reference state reveal closure failures. Disregistry analysis further shows that between the clusters of 4 and 5 rings a misfit dislocation belonging to set 1 shifts by one atomic plane from the Cu-Nb interface into the neighboring Cu layer, converting a small patch of the interface from KS_1 to KS_2, as shown in Figs. 2(b) and 2(d). Interface reconstructions analogous to those in Fig. 2 are also seen upon atom removal or insertion in Cu$^\alpha$ of KS_2, except that the affected interface patch is converted into KS_1 by the shifting of a set 1 dislocation segment from Cu-Cu$^\alpha$ into Cu-Nb.

The arrangements in Figs. 2(b) and 2(d) are actually pairs of extended jogs [14,15] separated by distance $h \approx 7.5$ Å. The topology of their creation is represented in Fig. 3. A compact point defect can be viewed as a dislocation loop of atomic dimensions, as in Fig. 3(a). If two edge line sections located on opposite sides of the loop glide apart then additional lengths of screw dislocation are created, as in Fig. 3(b). For an isolated loop, such expansion would be energetically unfavorable due to the creation of these extra screw segments unless it were to occur in the vicinity of an existing screw dislocation—e.g., a set 1 misfit dislocation in KS_1 or KS_2—with Burgers vector opposite to that of the loop, as in Fig. 3(c). One screw segment would then annihilate with the adjacent section of the preexisting dislocation giving the lower energy arrangement in Fig. 3(d). The configuration of a set 1 misfit dislocation relative to set 2 dislocations after absorbing a point defect is illustrated schematically in Fig. 3(e).

Insofar as they arise from atom removal or insertion, the extended jog pairs described above are the interfacial analogues of vacancies and interstitials in perfect crystals. Nevertheless, because their creation requires the reconstruction of a finite interface area with diameter approximately equal to the jog separation h, these jog pairs cannot be described as "point" defects. Indeed, they arise from

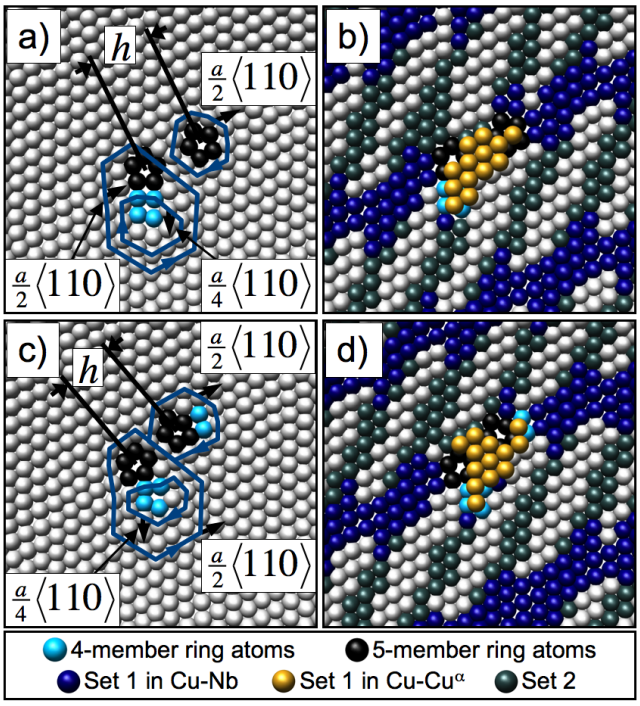

FIG. 2 (color online). Extended jog pair formation in the KS_1 interfacial Cu plane upon atom (a),(b) removal and (c),(d) insertion.

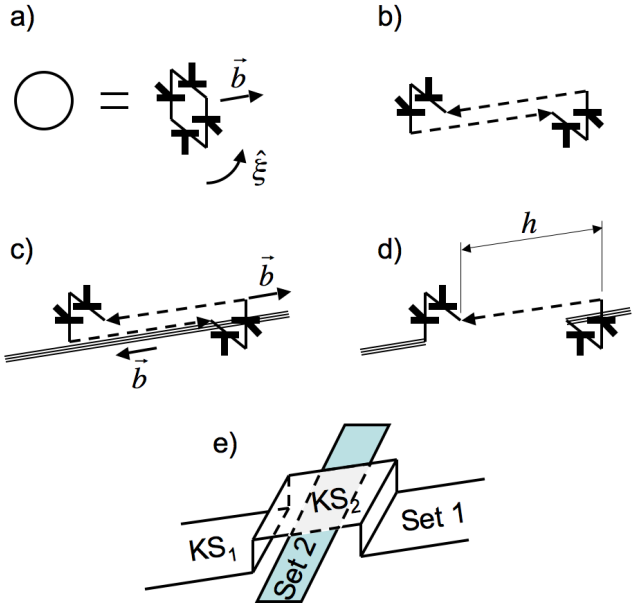

FIG. 3 (color online). The mechanisms of the reconstruction of point defects into jog pairs (see text).

the delocalization of point defects within the interface. Thus, rather than report the "formation energies" of jog pairs, it is more appropriate to specify the dependence of Cu-Nb interface energy $\gamma_{\text{Cu-Nb}}$ (eV/Å^2) on the areal density ρ_{Cu} (atoms/Å^2) of the interfacial Cu atomic layer. This dependence—shown in Fig. 4—is found by an iterative search for the ground state of the Cu-Nb interface at $T = 0$ K [16]. Interface Cu atoms are removed from different sites until a site with negative removal energy ΔE_{rem} is found. The interface with that atom removed is taken as the new starting point for the determination of ΔE_{rem} and the process is continued until a configuration is reached with no negative ΔE_{rem} sites. Values of $\gamma_{\text{Cu-Nb}}$ and ρ_{Cu} are computed after each successful removal. This procedure is applied using both KS_1 and KS_2 as starting configurations. Interface structures are relaxed using the same molecular dynamics annealing and potential energy minimization scheme as applied to the individual removal or insertion operations illustrated in Fig. 2. To estimate $\gamma_{\text{Cu-Nb}}$ at values of ρ_{Cu} below the ground state configuration, the above scheme is modified so atoms are removed from sites with $\Delta E_{\text{rem}} < 0.14$ eV and later with $\Delta E_{\text{rem}} < 0.43$ eV.

For $\rho_{\text{Cu}} \in (0.165, 0.171)$, $\gamma_{\text{Cu-Nb}}$ can be fitted as $\gamma_{\text{Cu-Nb}} = 72.499\rho_{\text{Cu}}^2 - 24.4405\rho_{\text{Cu}} + 2.0938$. Remarkably, its minimum value occurs at $\rho_{\text{Cu}}^{\text{min}} \approx 0.168$ atoms/Å^2, corresponding to an effective vacancy concentration in the Cu interface layer of ~5% compared to a perfect Cu {111} plane ($\rho_{\text{Cu}}^{\{111\}} \approx 0.177$ atoms/Å^2). The minimum interface energy configuration is termed KS_{min} and is shown in Fig. 1(c). It contains numerous jogs—causing set 1 dislocations to weave along their entire length between two adjacent atomic planes—and resembles certain epitaxial monolayer reconstructions [17–19]. An effective defect energy ΔE_{eff} (eV/atom) of removal or insertion of an area fraction c of atoms in the interfacial Cu layer in KS_{min} can be computed using the expression for $\gamma_{\text{Cu-Nb}}$: $\Delta E_{\text{eff}} = \Delta\gamma_{\text{Cu-Nb}}/|\Delta\rho_{\text{Cu}}| \approx 12|c|$eV/atom, where $\Delta\gamma_{\text{Cu-Nb}} = \gamma_{\text{Cu-Nb}}((1+c)\rho_{\text{Cu}}^{\text{min}}) - \gamma_{\text{Cu-Nb}}(\rho_{\text{Cu}}^{\text{min}})$ and $\Delta\rho_{\text{Cu}} = c\rho_{\text{Cu}}^{\text{min}}$. Thus, for a 1% density fluctuation

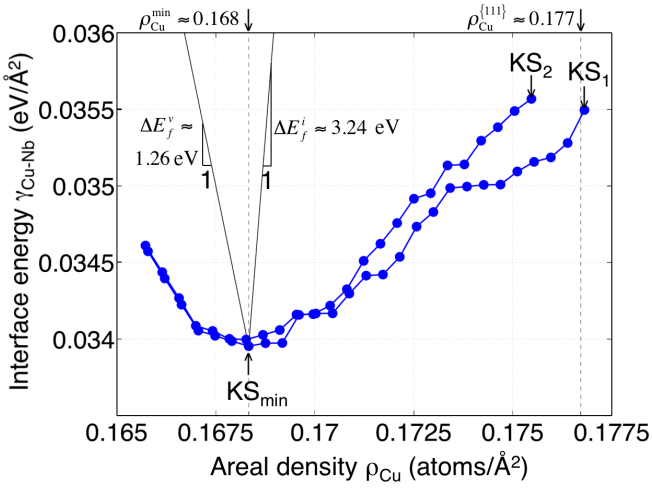

FIG. 4 (color online). Interface energy $\gamma_{\text{Cu-Nb}}$ (eV/Å^2) dependence on areal density ρ_{Cu} (atoms/Å^2) of interfacial Cu compared to Cu vacancy ΔE_f^v and interstitial ΔE_f^i formation energies.

$\Delta E_{\text{eff}} \approx 0.12$ eV, i.e., 1 order of magnitude smaller than the formation energies of vacancies ($\Delta E_f^v = 1.26$ eV) or interstitials ($\Delta E_f^i = 3.24$ eV) in fcc Cu. Because Cu-Nb interfaces can accommodate such large density fluctuations with minimal change in energy, they are virtually inexhaustible sinks for vacancies and interstitials produced by particle radiation.

Furthermore, unlike vacancies and interstitials, jog pairs have dipolar elastic fields, allowing two or more of them to undergo strong elastic interactions over distances comparable to the dipole dimension h. The critical distance for annihilation of a jog pair formed by removal of an atom and another arising from atom insertion is therefore markedly larger than that of a vacancy and interstitial in fcc Cu, which typically attract each other only within about one nearest neighbor separation. To measure the annihilation enhancement provided by interfaces let $\Delta E_{\text{ins-rem}}$ be the change in energy if an atom is inserted at $\vec{r}_{\text{ins}}$ and some other atom removed at $\vec{r}_{\text{rem}}$. If $\Delta E_{\text{ins-rem}} \leq \varepsilon = 0.1$ eV then the jog pairs due to removal and insertion are said to have recombined. For a given $\vec{r}_{\text{ins}}$, the critical distance Δr_c for recombination is the envelope of maximum $\Delta r = |\vec{r}_{\text{ins}} - \vec{r}_{\text{rem}}|$ values for all $\vec{r}_{\text{rem}}$. It is found that $\Delta r_c \approx 14$ Å $\approx 2h$ in KS_1, KS_2, and KS_{min}. Cu-Nb interfaces are therefore catalysts for efficient recombination of radiation-induced Frenkel pairs.

To accommodate atom removal or addition by the formation of jog pairs interface misfit dislocations must be able to reside in at least two adjacent planes. Otherwise, the arrangement shown in Fig. 3(d) could never have lower energy than a compact point defect. Thus, since neither set 1 nor set 2 misfit dislocations can reside in the Nb layer the formation of jog pairs has not been observed there. Cu-Nb interfaces may nevertheless still reduce radiation damage in the neighboring Nb since Nb vacancies and interstitials can lower their energies by jumping into the interfacial Cu plane, where they reconstruct into jog pairs and undergo enhanced recombination just like Frenkel pairs from Cu. The asymmetry in behavior of misfit dislocations with respect to Cu and Nb is attributed to the stacking fault properties of these materials. Although not a conventional fault configuration, the Cu-Cu$^{\alpha}$ interface in KS_2 may be viewed as a type of generalized stacking fault found between Cu {111} planes [20]. On the other hand, bcc materials like Nb are known not to support any stable fault configuration between {110} planes [14,21].

Interface geometry plays a central role among the factors that govern the properties of Cu-Nb interfaces: it determines the arrangement of interface misfit dislocations and the elastic distortion associated with the strained interfacial layer Cu$^{\alpha}$. Along with quantities like elastic constants and stacking fault energies, it may be used to estimate the likelihood of formation of analogous configurations in interfaces between materials other than Cu or Nb. Interfaces whose structures and point defect behaviors resemble those seen in Cu-Nb form a class of radiation damage-reducing interfaces that could be incorporated into nanocomposites designed for use in next generation nuclear reactors [22]. Understanding of interface structure can also be used to study the mechanical [5–7], elastic [23], and thermal behavior [24] of Cu-Nb multilayer nanocomposites and related materials.

We have shown that there is no such thing as a "point defect" in Cu-Nb interfaces, even though the neighboring material is crystalline. Instead, pairs of extended jogs with low effective formation energies and long-range interactions arise from atom removal or insertion, enabling these interfaces to reduce radiation damage.

We thank M. I. Baskes for insightful discussions. This research was funded by the LANL Directed Research and Development Program and the Director's Postdoctoral progam.

*Corresponding author.
demkowicz@lanl.gov

[1] A. P. Sutton and R. W. Balluffi, *Interfaces in Crystalline Materials* (Oxford University Press, Oxford, U.K., 1995).
[2] R. G. Hoagland *et al.*, Philos. Mag. A **82**, 643 (2002).
[3] M. J. Demkowicz *et al.*, Philos. Mag. **87**, 4253 (2007).
[4] A. K. Mukherjee, Mater. Sci. Eng. A **322**, 1 (2002).
[5] Y. C. Wang, A. Misra, and R. G. Hoagland, Scr. Mater. **54**, 1593 (2006).
[6] N. A. Mara *et al.*, Thin Solid Films **515**, 3241 (2007).
[7] A. Misra and R. G. Hoagland, J. Mater. Sci. **42**, 1765 (2007).
[8] T. Hochbauer *et al.*, J. Appl. Phys. **98**, 123516 (2005).
[9] A. Misra *et al.*, JOM **59**, 62 (2007).
[10] G. S. Was, *Fundamentals of Radiation Materials Science* (Springer, Berlin, 2007).
[11] P. M. Anderson *et al.*, Acta Mater. **51**, 6059 (2003).
[12] M. J. Demkowicz and R. G. Hoagland, J. Nucl. Mater. **372**, 45 (2008).
[13] M. S. Daw and M. I. Baskes, Phys. Rev. B **29**, 6443 (1984).
[14] J. P. Hirth and J. Lothe, *Theory of Dislocations* (Wiley, New York, 1982).
[15] P. B. Hirsch, Philos. Mag. **7**, 67 (1962).
[16] D. P. Landau and K. Binder, *A Guide to Monte Carlo Simulations in Statistical Physics* (Cambridge University Press, Cambridge, U.K., 2005).
[17] J. Jacobsen *et al.*, Phys. Rev. Lett. **75**, 489 (1995).
[18] I. Meunier *et al.*, Phys. Rev. B **59**, 10 910 (1999).
[19] B. V. Andryushechkin *et al.*, Surf. Sci. **488**, L541 (2001).
[20] H. van Swygenhoven, P. M. Derlet, and A. G. Froseth, Nat. Mater. **3**, 399 (2004).
[21] V. Vitek, Cryst. Lattice Defects **5**, 1 (1974).
[22] "Basic Research Needs for Advanced Nuclear Energy Systems," edited by J. Roberto and T. Diaz de la Rubia, DOE Office of Science, http://www.science.doe.gov/bes/reports/files/ANES_rpt.pdf.
[23] A. Fartash *et al.*, Phys. Rev. B **44**, 13 760 (1991).
[24] A. Misra, R. G. Hoagland, and H. Kung, Philos. Mag. **84**, 1021 (2004).